Physics of Fluids

Lubrication solution of the flow of a Herschel-Bulkley fluid with pressure-dependent rheological parameters in an asymmetric channel

Cite as: Phys. Fluids **31**, 023106 (2019); https://doi.org/10.1063/1.5087654
Submitted: 03 January 2019 . Accepted: 03 February 2019 . Published Online: 25 February 2019

Pandelitsa Panaseti, Georgios C. Georgiou, and Iasonas Ioannou

Physics of Fluids ARTICLE scitation.org/journal/phf

Lubrication solution of the flow of a Herschel-Bulkley fluid with pressure-dependent rheological parameters in an asymmetric channel

Cite as: Phys. Fluids 31, 023106 (2019); doi: 10.1063/1.5087654
Submitted: 3 January 2019 • Accepted: 3 February 2019 •
Published Online: 25 February 2019

Pandelitsa Panaseti,[1] Georgios C. Georgiou,[1,a)] and Iasonas Ioannou[2,b)]

AFFILIATIONS

[1] Department of Mathematics and Statistics, University of Cyprus, P.O. Box 20537, 1678 Nicosia, Cyprus
[2] Department of Mechanical and Process Engineering, ETH Zurich, Sonneggstrasse 3, 8092 Zurich, Switzerland

[a)] **Author to whom correspondence should be addressed:** georgios@ucy.ac.cy. **Tel.:** +357292612. **Fax:** +35722895352.
[b)] **E-mail:** iasonasce@gmail.com

ABSTRACT

The lubrication flow of a Herschel-Bulkley fluid in a long asymmetric channel, the walls of which are described by two arbitrary functions $h_1(x)$ and $h_2(x)$ such that $h_1(x) < h_2(x)$ and $h_1(x) + h_2(x)$ are linear, is solved extending a recently proposed method, which avoids the lubrication paradox approximating satisfactorily the correct shape of the yield surface at zero order [P. Panaseti *et al.*, "Pressure-driven flow of a Herschel-Bulkley fluid with pressure-dependent rheological parameters," Phys. Fluids **30**, 030701 (2018)]. Both the consistency index and the yield stress are assumed to be pressure-dependent. Under the lubrication approximation, the pressure at zero order is a function of x only, is decoupled from the velocity components, and obeys a first-order integro-differential equation. An interesting feature of the asymmetric flow is that the unyielded core moves not only in the main flow direction but also in the transverse direction. Explicit expressions for the two yield surfaces defining the asymmetric unyielded core are obtained, and the two velocity components in both the yielded and unyielded regions are calculated by means of closed-form expressions in terms of the calculated pressure and the two yield surfaces. The method is applicable in a range of Bingham numbers where the unyielded core extends from the inlet to the outlet plane of the channel. Semi-analytical solutions are derived in the case of an asymmetric channel with $h_1 = 0$ and linearly varying h_2. Representative results demonstrating the effects of the Bingham number and the consistency-index and yield-stress growth numbers are discussed.

I. INTRODUCTION

In a recent study,[1] we have extended a lubrication approximation method proposed by Fusi *et al.*[2] for solving pressure-driven flow of a Bingham-plastic in a symmetric channel, in order to solve the flow of a Herschel-Bulkley fluid with pressure-dependent consistency index k^* and yield stress τ_y^*. Thus, we have employed the following constitutive equation

$$\begin{cases} \mathbf{D}^* = \mathbf{0}, & \tau^* \le \tau_y^* \\ \boldsymbol{\tau}^* = 2\left(\frac{\tau_y^*}{\dot{\gamma}^*} + k^*\dot{\gamma}^{*n-1}\right)\mathbf{D}^*, & \tau^* > \tau_y^* \end{cases}, \tag{1}$$

where $\boldsymbol{\tau}^*$ is the viscous stress tensor,

$$\mathbf{D}^* \equiv \frac{1}{2}\left[\nabla^*\mathbf{v}^* + (\nabla^*\mathbf{v}^*)^T\right] \tag{2}$$

is the rate of deformation tensor, $\mathbf{v}^*$ is the velocity vector, $\dot{\gamma}^* \equiv \sqrt{2\mathrm{tr}\mathbf{D}^{*2}}$ and $\tau^* \equiv \sqrt{\mathrm{tr}\boldsymbol{\tau}^{*2}/2}$ are the magnitudes of $2\mathbf{D}^*$ and $\boldsymbol{\tau}^*$, respectively, and n is the power-law exponent. It should be noted that throughout this paper, symbols with stars denote dimensional quantities. As mentioned above, the consistency index and the yield stress are pressure dependent such that

$$k^*(p^*) = k_0^* f(\alpha^*(p^* - p_0^*)) \tag{3}$$

and

$$\tau_y^*(p^*) = \tau_0^*\, g(\beta^*(p^* - p_0^*)), \tag{4}$$

where k_0^* and τ_0^* are the consistency index and the yield stress at a reference pressure p_0^* (assumed to be the same for both material parameters) and f and g are appropriate functions such that $f(0) = g(0) = 1$. For example, $f(x) = e^x$ and $f(x) = 1 + x$ describe, respectively, exponential and linear variations of the consistency index with pressure, the latter case corresponding to the Barus formula for the viscosity.[3] Function f is increasing, while g can be either decreasing or increasing. The pressure dependence of the yield stress and the viscosity is well established in the mechanics of granular materials[4] and in oil-drilling fluids.[5] The reader is referred to Ref. 1 for a detailed literature review of experimental data on yield-stress materials with pressure-dependent rheological parameters.

Fusi *et al.* presented a novel technique for modeling the lubrication flow of a Bingham plastic (with constant rheological parameters) in a two-dimensional channel of non-uniform thickness.[2] This is based on the application of Reynolds transport theorem over the unyielded core. The advantage of the method is that it avoids the lubrication paradox and predicts at zero order the correct shape of the yield surface, whose behavior is opposite to that of the wall function, i.e., the width of the unyielded core increases when the channel width is reduced and vice versa. With other lubrication-approximation methods, the correct shape of the yield surface is obtained only at higher orders.[6,7] A limitation of the method of Fusi *et al.*,[2] however, is that it applies only when the unyielded region (plug) extends continuously from the inlet to the outlet plane, i.e., it is not applicable when the plug is broken.

Panaseti *et al.*[1] extended the method of Fusi *et al.*[2] to solve the lubrication flow of a Herschel-Bulkley fluid with pressure-dependent consistency index and yield stress. For the case of a channel of constant width, they demonstrated that the width of the unyielded core is also constant, despite the pressure dependence of the yield stress, and that the pressure distribution is not affected by the yield-stress function. They also derived analytical solutions for certain choices of the functions f and g corresponding to linear or exponential pressure-dependence of the two rheological parameters. Subsequently, Housiadas *et al.*[8] considered the axisymmetric flow following the approach proposed by Fusi and Farina[9] and assuming that both the plastic viscosity and the yield stress vary linearly with the total pressure. They calculated the total pressure and the radius of the unyielded core solving numerically the resulting nonlinear system of an ordinary differential equation (ODE) and an algebraic one. Their calculations revealed that the variation of the radius of the central unyielded core depends on the relative values of α^* and β^*. The latter contracts when $\beta^* < \alpha^*$, expands when $\beta^* > \alpha^*$, and remains cylindrical when $\beta^* = \alpha^*$. More recently, Fusi[10] revisited the symmetric planar flow problem assuming that the flow is driven by a prescribed inlet flux and not by a given pressure drop. In this case, the mathematical problem is much simpler reducing to a full nonlinear algebraic equation for the plug speed.

The objectives of the present work are: (a) to apply the method of Fusi *et al.*[2] in order to solve the lubrication flow of a Herschel-Bulkley fluid with pressure-dependent consistency index and yield stress in an asymmetric channel and (b) to derive analytical solutions for certain limiting cases, such as the flow in an asymmetric channel of linearly varying width.

The governing equations and the lubrication method are presented in Sec. II, where the zero-order solution is derived semi-analytically, in the sense that closed-form expressions are obtained for the positions of the upper and lower yield surfaces and for the two velocity components in terms of the pressure, which is found by solving a first-order integro-differential equation numerically. In Sec. III, the equations for a symmetric channel are outlined and the analytical solutions for a flat channel are provided for different functions describing the pressure-dependence of the consistency index and the yield stress. In Sec. IV, we derive analytical solutions for the case of an asymmetric channel with linearly changing width and for special forms of the functions describing the variation of the consistency index and the yield stress with pressure. The symmetric channel constitutes a special case of the derived solution. In Sec. V, representative results demonstrating the effects of the Bingham number and the consistency-index and yield-stress growth parameters are presented and discussed. Finally, in Sec. VI, concluding remarks are provided and some possibilities for further research are discussed.

II. ANALYSIS OF LUBRICATION FLOW

Consider the pressure-driven flow of an incompressible Herschel-Bulkley fluid in an asymmetric long channel of length L^* and variable width $h_2^*(x^*)$–$h_1^*(x^*)$, where $h_1^*(x)$ and $h_2^*(x)$ are the lower and upper wall functions, respectively, as illustrated in Fig. 1. A pressure p_{in}^* is applied at the inlet of the channel ($x^* = 0$), while the pressure at the exit ($x^* = L^*$) is $p_{out}^* < p_{in}^*$,

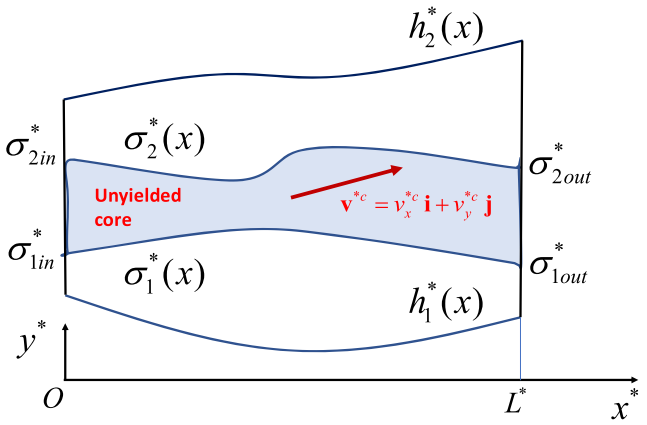

FIG. 1. Geometry and boundary conditions for the dimensional flow in an asymmetric channel of length L^* and variable width $h_2^*(x^*) - h_1^*(x^*)$. The unyielded core extends from the inlet to the outlet plane and is bounded by the two yield surfaces $\sigma_1^*(x^*)$ and $\sigma_2^*(x^*)$.

i.e., the imposed pressure difference is $\Delta p^* = p^*_{in} - p^*_{out} > 0$, and thus the flow is from the left to the right. Without loss of generality, we assume here that p^*_{out} is the reference pressure that appears in Eqs. (3) and (4), i.e., $p^*_{out} = p^*_0$. The main flow is in the x^* direction, while the z^*–velocity component is zero. Hence, the velocity vector is of the form $\mathbf{v}^* = v^*_x(x^*, y^*)\mathbf{i} + v^*_y(x^*, y^*)\mathbf{j}$. As illustrated in Fig. 1, the flow domain is thus divided into a lower and an upper yielded region and a central unyielded region defined by two unknown yield surfaces: $\sigma^*_1(x^*)$ and $\sigma^*_2(x^*)$, where $h^*_1(x^*) < \sigma^*_1(x^*) < \sigma^*_2(x^*) < h^*_2(x^*)$. The unyielded region extends from the inlet to the outlet plane, i.e., the plug is not broken. Let also $\sigma^*_{1in} \equiv \sigma^*_1(0)$, $\sigma^*_{1out} \equiv \sigma^*_1(L^*)$, $\sigma^*_{2in} \equiv \sigma^*_2(0)$, and $\sigma^*_{2out} \equiv \sigma^*_2(L^*)$.

For convenience, we will work with the dimensionless equations. We assume that the length L^* of the channel is much greater than say the channel width or half-width at the inlet H^* ($L^* \gg H^*$) and use the aspect ratio

$$\varepsilon \equiv \frac{H^*}{L^*} \ll 1 \tag{5}$$

to apply the classical lubrication approximation or thin-film approach.[6] The flow problem is dedimensionalised by scaling x^* by L^*, y^*, h^*_i, and σ^*_i by H^*, $(p^* - p^*_{out})$ by Δp^*, v^*_x by $H^*(\varepsilon\Delta p^*/k^*_0)^{1/n}$, v^*_y by $\varepsilon H^*(\varepsilon\Delta p^*/k^*_0)^{1/n}$, and the stress components by $\varepsilon\Delta p^*$. The dimensionless forms of the continuity equation and the two components of the momentum equation are as follows:

$$\frac{\partial v_x}{\partial x} + \frac{\partial v_y}{\partial y} = 0, \tag{6}$$

$$\varepsilon^{2/n-1}\mathrm{Re}\left(v_x\frac{\partial v_x}{\partial x} + v_y\frac{\partial v_x}{\partial y}\right) = -\frac{\partial p}{\partial x} + \varepsilon\frac{\partial \tau_{xx}}{\partial x} + \frac{\partial \tau_{yx}}{\partial y}, \tag{7}$$

$$\varepsilon^{2/n+1}\mathrm{Re}\left(v_x\frac{\partial v_y}{\partial x} + v_y\frac{\partial v_y}{\partial y}\right) = -\frac{\partial p}{\partial y} + \varepsilon^2\frac{\partial \tau_{yx}}{\partial x} + \varepsilon\frac{\partial \tau_{yy}}{\partial y}, \tag{8}$$

where all variables are dimensionless (notice that there are no stars) and Re is the Reynolds number defined by

$$\mathrm{Re} \equiv \frac{\rho^* H^{*3}\Delta p^{*2/n-1}}{k_0^{*2/n}L^*}, \tag{9}$$

with ρ^* being the constant density of the material. The nonzero components of the stress tensor in the yielded regime $\{(x,y):\ x\in[0,1],\ y\in[h_1,\sigma_1]\cup[\sigma_2,h_2]\}$ read

$$\left.\begin{aligned}
\tau_{xx} &= 2\varepsilon\left[\frac{\mathrm{Bn}\,g(\beta p)}{\dot\gamma} + f(\alpha p)\dot\gamma^{n-1}\right]\frac{\partial v_x}{\partial x}\\
\tau_{yx} &= \left[\frac{\mathrm{Bn}\,g(\beta p)}{\dot\gamma} + f(\alpha p)\dot\gamma^{n-1}\right]\left(\frac{\partial v_x}{\partial y} + \varepsilon^2\frac{\partial v_y}{\partial x}\right)\\
\tau_{yy} &= 2\varepsilon\left[\frac{\mathrm{Bn}\,g(\beta p)}{\dot\gamma} + f(\alpha p)\dot\gamma^{n-1}\right]\frac{\partial v_y}{\partial y}
\end{aligned}\right\},\quad y\in[h_1,\sigma_1]\cup[\sigma_2,h_2], \tag{10}$$

where

$$\dot\gamma = \sqrt{4\varepsilon^2\left(\frac{\partial v_x}{\partial x}\right)^2 + \left(\frac{\partial v_x}{\partial y} + \varepsilon^2\frac{\partial v_y}{\partial x}\right)^2}. \tag{11}$$

In Eq. (10), there appear three dimensionless numbers, the Bingham number Bn and the consistency-index and yield-stress growth numbers a and β, which are defined by

$$\mathrm{Bn} \equiv \frac{\tau^*_0}{\varepsilon\Delta p^*}, \quad \alpha \equiv a^*\Delta p^*, \quad \beta \equiv \beta^*\Delta p^*. \tag{12}$$

It is clear that when g is an increasing function, the dimensionless yield stress is reduced from the inlet plane to the outlet plane.

The unyielded core, defined by $\Omega = \{(x,y):\ x\in[0,1],\ y\in[\sigma_1,\sigma_2]\}$, moves as a solid, i.e., at a constant velocity $\mathbf{v}^c = v^c_x\mathbf{i} + v^c_y\mathbf{j}$. Thus,

$$v_x = v^c_x \quad \text{and} \quad v_y = v^c_y \quad \text{for} \quad \sigma_1(x) \le y \le \sigma_2(x). \tag{13}$$

Remark 1. The transverse velocity of the unyielded core becomes zero only in the symmetric case.

For steady-state flow in the absence of body forces, the integral balance of linear momentum of the whole plug core yields the following equation:[1,2]

$$\int_0^1 \left\{\left[-\sigma_{2x}(-p+\varepsilon\tau_{xx}) + \tau_{yx}\right]_{y=\sigma_2} - \left[-\sigma_{1x}(-p+\varepsilon\tau_{xx}) + \tau_{yx}\right]_{y=\sigma_1}\right\}dx + (\sigma_{2in} - \sigma_{1in})p_{in} = 0, \tag{14}$$

where $\sigma_{ix} \equiv d\sigma_i/dx$, $i = 1,2$. Finally, the dimensionless pressure satisfies the following boundary conditions:

$$p(0,\sigma_{1in}) = p(0,\sigma_{2in}) = 1, \quad p(1,\sigma_{1out}) = p(1,\sigma_{2out}) = 0. \tag{15}$$

A. The zero-order problem

As in our previous studies,[1,8] we solve the zero-order problem. For the sake of simplicity, we will avoid introducing new symbols for the zero-order variables. At zero order, the y-component of the momentum equation is simplified to $\partial p/\partial y = 0$ and thus $p = p(x)$. The continuity and x-momentum equations at zero order then read as follows:

$$\frac{\partial v_x}{\partial x} + \frac{\partial v_y}{\partial y} = 0, \tag{16}$$

$$-\frac{\partial p}{\partial x} + \frac{\partial \tau_{yx}}{\partial y} = 0. \tag{17}$$

Moreover, $\tau_{xx} = \tau_{yy} = 0$, while the shear stress component is given by

$$\tau_{yx} = \left[\frac{\mathrm{Bn}g(\beta p)}{\dot\gamma} + f(\alpha p)\dot\gamma^{n-1}\right]\frac{\partial v_x}{\partial y}, \quad y\in[h_1,\sigma_1]\cup[\sigma_2,h_2]. \tag{18}$$

In the lower yielded region, $\dot{\gamma} = |\partial v_x/\partial y| = \partial v_x/\partial y$ and thus

$$\tau_{yx} = Bng(\beta p) + f(\alpha p)\left(\frac{\partial v_x}{\partial y}\right)^n, \quad y \in [h_1, \sigma_1]. \tag{19}$$

Substituting the above expression into the x-momentum Eq. (17), integrating twice, and applying the boundary conditions $v_x(x, h_1) = \partial v_x/\partial y(x, \sigma_1) = 0$, the following expression is obtained for v_x:

$$v_x(x, y) = \left[1 - \frac{(\sigma_1 - y)^{1+1/n}}{(\sigma_1 - h_1)^{1+1/n}}\right] v_x^c, \quad y \in [h_1, \sigma_1], \tag{20}$$

where

$$v_x^c = \frac{(-p_x)^{1/n}(\sigma_1 - h_1)^{1+1/n}}{(1+1/n) f^{1/n}(\alpha p)} \tag{21}$$

and $p_x \equiv dp/dx$. Similarly, in the upper yielded region where $\dot{\gamma} = |\partial v_x/\partial y| = -\partial v_x/\partial y$, the shear stress is given by

$$\tau_{yx} = -Bng(\beta p) - f(\alpha p)\left(-\frac{\partial v_x}{\partial y}\right)^n, \quad y \in [\sigma_2, h_2]. \tag{22}$$

Substituting in the momentum equation, integrating twice, and applying the boundary conditions $\partial v_x/\partial y(x, \sigma_2) = v_x(x, h_2) = 0$, one gets

$$v_x(x, y) = \left[1 - \frac{(y - \sigma_2)^{1+1/n}}{(h_2 - \sigma_2)^{1+1/n}}\right] v_x^c, \quad y \in [\sigma_2, h_2], \tag{23}$$

where

$$v_x^c = \frac{(-p_x)^{1/n}(h_2 - \sigma_2)^{1+1/n}}{(1+1/n) f^{1/n}(\alpha p)}. \tag{24}$$

Since the core velocity is constant, the pressure satisfies the first-order ODEs defined by

$$\frac{p_x}{f(\alpha p)}(\sigma_1 - h_1)^{n+1} = \frac{p_x}{f(\alpha p)}(h_2 - \sigma_2)^{n+1} = -(1+1/n)^n (v_x^c)^n. \tag{25}$$

The pressure p and the core velocity v_x^c can be determined upon integration and application of the two conditions for p,

$$p(0) = 1, \quad p(1) = 0. \tag{26}$$

The transverse velocity component in the lower and upper yielded regions is found by integrating the continuity equation (16) and applying the no-penetration boundary condition at the two walls, $v_y(x, h_1) = v_y(x, h_2) = 0$,

$$\left.\begin{aligned} v_y &= -\int_{h_1}^{y} \frac{\partial v_x}{\partial x}\, dy, \quad y \in [h_1, \sigma_1] \\ v_y &= \int_{y}^{h_2} \frac{\partial v_x}{\partial x}\, dy, \quad y \in [\sigma_2, h_2] \end{aligned}\right\}. \tag{27}$$

Substituting v_x from Eq. (20) into Eq. (27) and carrying out the required differentiation and integration, one gets for the lower yielded region

$$v_y = \frac{v_x^c}{2+1/n}\left[\sigma_{1x} + (1+1/n)h_{1x} - (2+1/n)\left(\frac{\sigma_1 - y}{\sigma_1 - h_1}\right)^{1+1/n} \times \sigma_{1x} + (1+1/n)(\sigma_{1x} - h_{1x})\left(\frac{\sigma_1 - y}{\sigma_1 - h_1}\right)^{2+1/n}\right], \quad y \in [h_1, \sigma_1], \tag{28}$$

where $h_{1x} \equiv dh_1/dx$. The satisfaction of condition $v_y(x, \sigma_1) = v_y^c$ requires that

$$\sigma_{1x} + (1+1/n)h_{1x} = (2+1/n)\frac{v_y^c}{v_x^c}. \tag{29}$$

Combining Eqs. (28) and (29) and simplifying lead to the following expression for the transverse velocity in the lower yielded region:

$$v_y = v_y^c + \frac{(\sigma_1 - y)^{1+1/n}}{(\sigma_1 - h_1)^{2+1/n}}\left\{(1+1/n)(y - h_1)h_{1x}v_x^c - [\sigma_1 - h_1 + (1+1/n)(y - h_1)]v_y^c\right\}, \quad y \in [h_1, \sigma_1]. \tag{30}$$

Working similarly in the upper yielded region, one finds that

$$\sigma_{2x} + (1+1/n)h_{2x} = (2+1/n)\frac{v_y^c}{v_x^c} \tag{31}$$

and

$$v_y = v_y^c + \frac{(y - \sigma_2)^{1+1/n}}{(h_2 - \sigma_2)^{2+1/n}}\left\{(1+1/n)(h_2 - y)h_{2x}v_x^c - [h_2 - \sigma_2 + (1+1/n)(h_2 - y)]v_y^c\right\}, \quad y \in [\sigma_2, h_2], \tag{32}$$

where $h_{2x} \equiv dh_2/dx$.

We still need to find the equations corresponding to the unknown positions of the two yield surfaces. Since the unyielded core moves at constant velocity, $v_x(y = \sigma_1) = v_x(y = \sigma_2) = v_x^c$. Equating Eqs. (21) and (24) results in

$$\sigma_1 + \sigma_2 = h_1 + h_2. \tag{33}$$

Remark 2. Since $\sigma_1 - h_1 = h_2 - \sigma_2$, the widths of the lower and upper yielded regions are equal for any x.

Combining now Eqs. (29) and (31), we get

$$\sigma_{2x} - \sigma_{1x} = -\left(1 + \frac{1}{n}\right)(h_{2x} - h_{1x}). \tag{34}$$

Integrating the above equation with respect to x, we get the following expression for the thickness of the unyielded core:

$$\sigma_2(x) - \sigma_1(x) = -\left(1 + \frac{1}{n}\right)[h_2(x) - h_1(x)] + C, \tag{35}$$

where C is an unknown constant to be determined. From the system of Eqs. (33) and (35), we find that

$$\sigma_1(x) = -\frac{1}{2n}h_1(x) + \left(1 + \frac{1}{2n}\right)h_2(x) - \frac{C}{2} \tag{36}$$

and

$$\sigma_2(x) = \left(1 + \frac{1}{2n}\right)h_1(x) - \frac{1}{2n}h_2(x) + \frac{C}{2}. \tag{37}$$

Remark 3. The above results generalize those of Panaseti *et al.*[1] for a symmetric channel, in which case $v_y^c = 0$. The width of the unyielded core increases if the width of the channel decreases and vice versa. The variation of the width of the unyielded core is enhanced by shear thinning and is independent of the other material and flow parameters, which affect only the constant C. As noted in Ref. 1, reducing the power-law exponent n in a converging channel causes the plug to expand faster, which is expected, given that the velocity profile becomes flatter as shear thinning is enhanced.

Remark 4. From Eqs. (33) and (34), one observes that

$$\sigma_{1x} = \left(1 + \frac{1}{2n}\right) h_{2x} - \frac{1}{2n} h_{1x}, \tag{38}$$

which upon substitution into Eq. (29) yields

$$\frac{v_y^c}{v_x^c} = \frac{h_{1x} + h_{2x}}{2}. \tag{39}$$

Given that the LHS is constant, the solution derived above is valid, provided that $h_{1x} + h_{2x}$ is constant, or equivalently when the sum $h_1 + h_2$ is a linear function of x. This condition is satisfied when the channel is symmetric as well as when both the wall functions are linear. In the general case, for a given lower wall function, the upper wall function must be of the form

$$h_2(x) = -h_1(x) + c_1 x + c_2, \tag{40}$$

where c_1 and c_2 are constants.

Remark 5. If the width of the channel, $h_2(x) - h_1(x)$, is constant, then the two walls are flat (and parallel) and the width $\sigma_2(x) - \sigma_1(x)$ of the unyielded core is also constant.

Remark 6. It is easily shown that the constant C is related to the volumetric flow rate through the channel, for which we have

$$Q = \int_{h_1}^{h_2} v_x(x,y)\, dy = \int_{h_1}^{\sigma_1} v_x(x,y)\, dy + (\sigma_2 - \sigma_1) v_x^c + \int_{\sigma_2}^{h_2} v_x(x,y)\, dy, \tag{41}$$

where we took into account that the x-component of the velocity in the unyielded region is v_x^c. Substituting the velocity from Eqs. (20) and (23) for the lower and upper yielded regions and integrating, we obtain

$$Q = \frac{v_x^c}{2 + 1/n}[\sigma_2 - \sigma_1 + (1 + 1/n)(h_2 - h_1)]. \tag{42}$$

The expression within the brackets is the constant C of Eq. (35). Thus,

$$C = (2 + 1/n)\frac{Q}{v_x^c}. \tag{43}$$

Substituting into Eq. (37) and making use of Eq. (40), one finds

$$\sigma_2(x) = \left(1 - \frac{1}{2n}\right) c_1 x - \left(1 + \frac{1}{n}\right) h_2(x) + \left(1 + \frac{1}{2n}\right) \frac{Q}{v_x^c}. \tag{44}$$

To determine the constant C, we return to the plug momentum balance Eq. (14), which at zero order becomes

$$\int_0^1 \left\{ \left[-\sigma_{2x}(-p) + \tau_{yx} \right]_{y=\sigma_2} - \left[-\sigma_{1x}(-p) + \tau_{yx} \right]_{y=\sigma_1} \right\} dx + (\sigma_{2in} - \sigma_{1in}) p_{in} = 0. \tag{45}$$

From Eqs. (19) and (22), we get

$$\tau_{yx}\big|_{y=\sigma_1} = Bng(\beta p) \quad \text{and} \quad \tau_{yx}\big|_{y=\sigma_2} = -Bng(\beta p). \tag{46}$$

Substituting into Eq. (45), using integration by parts, and applying the boundary conditions (26), we find that

$$\int_0^1 (\sigma_2 - \sigma_1) p_x dx + 2Bn \int_0^1 g(\beta p) dx = 0. \tag{47}$$

Substituting Eq. (35) into Eq. (47) and integrating, one gets

$$C = 2Bn \int_0^1 g(\beta p)\, dx - (1 + 1/n) \int_0^1 p_x (h_2 - h_1)\, dx \tag{48}$$

or

$$C = 2Bn \int_0^1 g(\beta p)\, dx + (1 + 1/n) \left[h_{2in} - h_{1in} + \int_0^1 p(h_{2x} - h_{1x})\, dx \right]. \tag{49}$$

Substituting C from Eq. (49) into Eq. (36) yields

$$\sigma_1 = -Bn \int_0^1 g(\beta p)\, dx - \frac{1}{2n} h_1 + \left(1 + \frac{1}{2n}\right) h_2 - \frac{1}{2}(1 + 1/n) \left[h_{2in} - h_{1in} + \int_0^1 p(h_{2x} - h_{1x})\, dx \right]. \tag{50}$$

Finally, combining the above equation with Eq. (25), we get the following integro-differential equation:

$$p_x \left\{ -Bn \int_0^1 g(\beta p)\, dx + \left(1 + \frac{1}{2n}\right)(h_2 - h_1) - \frac{1}{2}(1 + 1/n) \times \left[h_{2in} - h_{1in} + \int_0^1 p(h_{2x} - h_{1x})\, dx \right] \right\}^{n+1} = Kf(\alpha p), \tag{51}$$

which is subject to conditions (26). Once the pressure is calculated, C, $\sigma_1(x)$, and $\sigma_2(x)$ are readily calculated from Eqs. (49), (36), and (37), respectively. The two velocity components can then be calculated by means of Eqs. (20) and (30) in the lower yielded region and Eqs. (23) and (32) in the upper yielded region. The two components of the velocity of the unyielded core are calculated by means of Eqs. (21) and (29). For the latter velocity component, we get

$$v_y^c = \frac{\sigma_{1x} + (1 + 1/n) h_{1x}}{(2 + 1/n)} v_x^c. \tag{52}$$

The velocity distributions in the asymmetric channel are thus given by

$$v_x(x,y) = v_x^c \begin{cases} 1 - \left(\frac{\sigma_1 - y}{\sigma_1 - h_1}\right)^{1+1/n}, & y \in [h_1, \sigma_1) \\ 1, & y \in [\sigma_1, \sigma_2] \\ 1 - \left(\frac{y - \sigma_2}{h_2 - \sigma_2}\right)^{1+1/n}, & y \in (\sigma_2, h_2] \end{cases} \tag{53}$$

and

$$v_y(x,y) = v_y^c + \begin{cases} \dfrac{(\sigma_1 - y)^{1+1/n}}{(\sigma_1 - h_1)^{2+1/n}}\left\{(1+1/n)(y-h_1)h_{1x}v_x^c - [\sigma_1 - h_1 + (1+1/n)(y-h_1)]v_y^c\right\}, & y \in [h_1, \sigma_1] \\ 0, & y \in [\sigma_1, \sigma_2] \\ \dfrac{(y - \sigma_2)^{1+1/n}}{(h_2 - \sigma_2)^{2+1/n}}\left\{(1+1/n)(h_2-y)h_{2x}v_x^c - [h_2 - \sigma_2 + (1+1/n)(h_2-y)]v_y^c\right\}, & y \in [\sigma_2, h_2] \end{cases} \tag{54}$$

It should be pointed out that in order for the present model to be applied, $Bn_{c1} \le Bn \le Bn_{c2}$, where Bn_{c1} is the critical value of the Bingham number at which the plug is broken ($\sigma_1 = \sigma_2$) and Bn_{c2} is the critical Bingham below which flow occurs, i.e., the Bingham number at which the core touches the walls and the flow ceases. If the plug is broken, which implies that $\sigma_1 = \sigma_2 = \sigma$ at some point x_c, then $2\sigma = h_1 + h_2$ and therefore the plug breaks in the middle of the channel at $x = x_c$. Equation (35) then gives

$$C_c = \left(1 + \frac{1}{n}\right)[h_2(x_c) - h_1(x_c)], \tag{55}$$

Substituting the above equation into Eq. (49) yields the critical Bingham number below which the plug is broken,

$$Bn_{c1} = \frac{\left(1+\frac{1}{n}\right)\left[h_2(x_c) - h_1(x_c) - h_{2in} + h_{1in} - \int_0^1 p(h_{2x} - h_{1x})\,dx\right]}{2\int_0^1 g(\beta p)dx}. \tag{56}$$

Now, if $\sigma_1 = h_1$ at any point x_w, then $\sigma_2(x_w) = h_2(x_w)$, i.e., the two unyielded surfaces touch the two walls at the same distance x_w downstream. In this case, there is obviously no flow and Eq. (35) gives

$$C_w = \left(2 + \frac{1}{n}\right)[h_2(x_w) - h_1(x_w)]. \tag{57}$$

The second critical value Bn_{c2} above which there is no flow coincides with the critical number at which there is no flow in a flat channel of width equal to the minimum width of the channel,

$$Bn_{c2} = \frac{(h_2 - h_1)_{\min}}{2\int_0^1 g(\beta p_F)dx}, \tag{58}$$

where p_F is the pressure corresponding to flow in the aforementioned flat channel.

III. FLOW IN A SYMMETRIC CHANNEL

The flow in a symmetric channel constitutes a special case of the flow problem analyzed in Sec. II. Letting

$$h(x) = -h_1(x) = h_2(x), \tag{59}$$

then Eqs. (36) and (37) yield

$$\sigma(x) = -\sigma_1(x) = \sigma_2(x). \tag{60}$$

Hence, Eq. (35) is simplified as follows:

$$\sigma(x) = -\left(1 + \frac{1}{n}\right)h(x) + \frac{C}{2}, \tag{61}$$

which also implies that

$$\sigma_x + (1+1/n)h_x = 0. \tag{62}$$

Hence, from Eq. (29) it is deduced that $v_y^c = 0$, as expected by symmetry. From Eq. (49), one finds that

$$\frac{C}{2} = Bn\int_0^1 g(\beta p)\,dx + (1+1/n)\left[h_{in} + \int_0^1 p h_x\,dx\right]. \tag{63}$$

Finally, from Eq. (25), we observe that the pressure satisfies the simplified equation

$$\frac{p_x}{f(\alpha p)} = -\frac{(1+1/n)^n (v_x^c)^n}{(h-\sigma)^{n+1}}. \tag{64}$$

After calculating the pressure, the constant C and the location of the yield surface $\sigma(x)$ are computed via Eqs. (63) and (61), respectively. The velocity above the symmetry plane is then given by

$$v_x(x,y) = v_x^c \begin{cases} 1, & y \in [0, \sigma] \\ 1 - \left(\dfrac{y-\sigma}{h-\sigma}\right)^{1+1/n}, & y \in (\sigma, h] \end{cases}, \tag{65}$$

where

$$v_x^c = \frac{(-p_x)^{1/n}(h-\sigma)^{1+1/n}}{(1+1/n)f^{1/n}(\alpha p)}. \tag{66}$$

The expressions (56) and (58) for the two critical Bingham numbers are simplified as follows:

$$Bn_{c1} = \frac{\left(1+\frac{1}{n}\right)\left[h(x_c) - h_{in} - \int_0^1 p h_x\,dx\right]}{\int_0^1 g(\beta p)dx} \tag{67}$$

and

$$Bn_{c2} = \frac{h_{\min}}{\int_0^1 g(\beta p_F)dx}. \tag{68}$$

Below we focus on the case of a flat channel with $h = 1$ and derive the complete analytical solutions for various combinations of the functions f and g, which describe the dependence of k and τ_0 on pressure. As noted in Panaseti *et al.*,[1] the

yield surface is flat despite the pressure dependence of the rheological parameters, given by

$$\sigma = \mathrm{Bn}\int_0^1 g(\beta p)\,dx. \tag{69}$$

The pressure satisfies the following first-order integro-differential equation:

$$\frac{p_x}{f(\alpha p)} = -\frac{(1+1/n)^n (v_x^c)^n}{(h-\sigma)^{n+1}} = -K', \tag{70}$$

where K' is an unknown constant. Solving the above equation and applying the boundary conditions (26) yield the pressure $p(x)$ and the constant K'. Then σ and the velocity $v_x(x,y)$ are computed by means of Eqs. (69) and (65), respectively, where

$$v_x^c = \frac{K'^{1/n}(1-\sigma)^{1+1/n}}{1+1/n}. \tag{71}$$

The analytical solutions for a Bingham-plastic ($n = 1$) with $f, g \in \{1, 1+x, e^x\}$ are tabulated in Table I. It is readily observed that the pressure is independent of the yield-stress growth function, which affects only the semi-width σ of the unyielded core. It turns out that only in the particular case where f is linear and g is exponential there is no analytical solution. From Eq. (69), it is deduced that for flow to occur, it must be $\sigma < 1$, and thus the critical number below which flow occurs is

$$\mathrm{Bn}_{c2} = \frac{1}{\int_0^1 g(\beta p)\,dx}. \tag{72}$$

It is also evident from Eq. (67) that in the case of a flat channel, Bn_{c1} vanishes.

TABLE I. Expressions for the pressure $p(x)$, the constant K', and the elevation of the yield surface σ for a Bingham-plastic ($n = 1$) and different forms of the consistency-index growth function f and the yield stress growth function g in the case of a symmetric flat channel of unit width ($h = 1$). The velocity is calculated by means of Eq. (65).

$f(\alpha p) = 1$	
$p(x) = 1 - x,\ K' = 1$	
$g(\beta p) = 1$	$\sigma = \mathrm{Bn}$
$g(\beta p) = 1 + \beta p$	$\sigma = \left(1 + \frac{\beta}{2}\right)\mathrm{Bn}$
$g(\beta p) = e^{\beta p}$	$\sigma = \frac{e^\beta - 1}{\beta}\mathrm{Bn}$
$f(\alpha p) = 1 + \alpha p$	
$p(x) = \frac{1}{\alpha}\left[(1+\alpha)^{1-x} - 1\right],\ K' = \frac{\ln(1+\alpha)}{\alpha}$	
$g(\beta p) = 1$	$\sigma = \mathrm{Bn}$
$g(\beta p) = 1 + \beta p$	$\sigma = \left[1 - \beta\left\{\frac{1}{\alpha} - \frac{1}{\ln(1+\alpha)}\right\}\right]\mathrm{Bn}$
$g(\beta p) = e^{\beta p}$	No analytical solution
$f(\alpha p) = e^{\alpha p}$	
$p(x) = \frac{1}{\alpha}\ln\frac{1}{(1-e^{-\alpha})x + e^{-\alpha}},\ K' = \frac{1-e^{-\alpha}}{\alpha}$	
$g(\beta p) = 1$	$\sigma = \mathrm{Bn}$
$g(\beta p) = 1 + \beta p$	$\sigma = \left[1 - \frac{\beta(1+\alpha+e^a)}{\alpha(e^a-1)}\right]\mathrm{Bn}$
$g(\beta p) = e^{\beta p}$	$\sigma = \begin{cases} \frac{a}{1-e^{-a}}\mathrm{Bn}, & \beta = \alpha \\ \frac{1-e^{\beta-\alpha}}{(1-\beta/a)(1-e^{-a})}\mathrm{Bn}, & \beta \neq \alpha \end{cases}$

IV. FLOW IN A CHANNEL WITH LINEARLY VARYING UPPER WALL

In this section, we consider the flow in a channel with walls described by

$$h_1 = 0, \quad h_2 = 1 + \Delta h x, \tag{73}$$

where Δh is a constant; hence, the upper wall may be diverging ($\Delta h > 0$), flat ($\Delta h = 0$), or converging ($\Delta h < 0$). The positions of the two yield surfaces [Eqs. (36) and (37)] are then simplified as follows:

$$\sigma_1(x) = \left(1 + \frac{1}{2n}\right)(1 + \Delta h x) - \frac{C}{2} \tag{74}$$

and

$$\sigma_2(x) = -\frac{1}{2n}(1 + \Delta h x) + \frac{C}{2}. \tag{75}$$

Therefore, $\sigma_1(x)$ is increasing, while $\sigma_2(x)$ is decreasing downstream in a diverging channel and vice versa in a converging channel. As shown in Sec. III and also in Ref. 1, in the symmetric case of a horizontal channel with two parallel walls, the two yield surfaces are also horizontal.

In order to simplify the resulting solution expressions for this particular flow, we introduce a constant A, replacing the constant C by means of

$$\mathrm{A} \equiv \frac{1}{\Delta h}\left(1 - \frac{C}{2+1/n}\right) \Leftrightarrow C = (2+1/n)(1 - \Delta h \mathrm{A}). \tag{76}$$

Equation (49) for this particular geometry gives

$$(2+1/n)(1-\Delta h \mathrm{A}) = 2\mathrm{Bn}\int_0^1 g(\beta p)dx + (1+1/n)\left(1 + \Delta h \int_0^1 p dx\right) \tag{77}$$

or

$$1 - [(2+1/n)\mathrm{A} + (1+1/n)\mathrm{I}(\mathrm{A})]\Delta h = 2\mathrm{Bn}\int_0^1 g(\beta p)dx, \tag{78}$$

where

$$\mathrm{I}(\mathrm{A}) \equiv \int_0^1 p\,dx. \tag{79}$$

Expressions (74) and (75) for the two yield surfaces now become

$$\sigma_1(x) = \left(1 + \frac{1}{2n}\right)\Delta h(\mathrm{A} + x) \tag{80}$$

and

$$\sigma_2(x) = 1 - \Delta h A - \frac{1}{2n}\Delta h(A + x). \tag{81}$$

In this case, ODE (25) for the pressure can be written as

$$\frac{p_x}{f(\alpha p)} = -\frac{K'}{(A + x)^{n+1}}, \tag{82}$$

where

$$K' = \frac{(1 + 1/n)^n (v_x^c)^n}{(1 + 1/2n)^{n+1}(\Delta h)^{n+1}}. \tag{83}$$

It is easily seen that once K' is calculated, the velocity of the unyielded core in the x-direction can be found,

$$v_x^c = \frac{[(1 + 1/2n)\Delta h]^{1+1/n} K'^{1/n}}{1 + 1/n}. \tag{84}$$

In the general case, for given functions f and g, the pressure $p(x)$ and the constant K' can be found by integrating Eq. (82) and applying the boundary conditions (26). The constant A is computed numerically solving Eq. (78) where the integral of the RHS as well as I(A) is also computed numerically. Then σ_1 and σ_2 are computed by means of Eqs. (80) and (81), respectively. The component v_x^c is given by Eq. (84), whereas from Eq. (29), we get

$$v_y^c = \frac{\sigma_{1x} + (1 + 1/n)h_{1x}}{2 + 1/n} v_x^c = \frac{(1 + 1/2n)\Delta h}{2 + 1/n} v_x^c \Rightarrow v_y^c = \frac{\Delta h}{2} v_x^c. \tag{85}$$

We observe that the ratio v_y^c/v_x^c depends only on Δh, i.e., it is independent of the material parameters. Finally, the two velocity components in the two yielded regimes are calculated by means of Eqs. (53) and (54).

Explicit expressions for the pressure $p(x)$ and the constant K' can be derived when the consistency-index growth function f is linear or exponential. These expressions are tabulated in Table II. It should be noted that the effects of the yield-stress growth parameter β and the Bingham number Bn are incorporated in the value of the constant A. The integral $I(A)$ can be calculated analytically only in the case where f is unity (constant consistency index),

$$I(A) = \begin{cases} A[(A + 1)\ln(1 + 1/A) - 1], & n = 1 \\ \dfrac{(A + 1)(1 + 1/A)^{n-1} - A - n}{(n - 1)\left[(1 + 1/A)^n - 1\right]}, & n \neq 1 \end{cases}. \tag{86}$$

An analytical expression for Eq. (78) can be derived only in the case of linear g, i.e., $g(\beta p) = 1 + \beta p$,

$$1 - [(2 + 1/n)A + (1 + 1/n)I(A)]\Delta h = 2Bn[1 + \beta I(A)]. \tag{87}$$

As noted above, the unyielded core expands downstream in the case of a converging channel and contracts in the diverging channel. As a result, the present lubrication method is applicable only in a range of Δh values,

$$(\Delta h)_{\min} < \Delta h < (\Delta h)_{\max}. \tag{88}$$

TABLE II. Analytical solutions for the pressure $p(x)$, the constant K', and v_x^c for a Herschel-Bulkley fluid and different forms of the consistency-index growth function f in the case of a channel with linearly varying wall ($h_1 = 0$, $h_2 = 1 + \Delta hx$). The constant A is computed numerically solving Eq. (78).

$f(\alpha p) = 1$	$K' = \dfrac{n}{1/A^n - 1/(A+1)^n}$	$p(x) = \dfrac{\left(\frac{A+1}{A+x}\right)^n - 1}{(1+1/A)^n - 1}$
	$v_x^c = \dfrac{n^{1/n}[(1+1/2n)\Delta h]^{1+1/n}}{(1+1/n)\left[1/A^n - 1/(A+1)^n\right]^{1/n}}$	
$f(\alpha p) = 1 + \alpha p$	$K' = \dfrac{n\ln(1+\alpha)/\alpha}{1/A^n - 1/(A+1)^n}$	$p(x) = \dfrac{1}{\alpha}\left\{(1+\alpha)^{\left[(A+1)^n/(A+x)^n - 1\right]/\left[(1+1/A)^n - 1\right]} - 1\right\}$
	$v_x^c = \dfrac{[(1+1/2n)\Delta h]^{1+1/n}}{1+1/n}\left[\dfrac{n\ln(1+\alpha)/\alpha}{1/A^n - 1/(A+1)^n}\right]^{1/n}$	
$f(\alpha p) = e^{\alpha p}$	$K' = \dfrac{n(1-e^{-\alpha})/\alpha}{1/A^n - 1/(A+1)^n}$	$p(x) = -\dfrac{1}{\alpha}\ln\left\{1 - (1-e^{-\alpha})\left[\left(\dfrac{A+1}{A+x}\right)^n - 1\right]/\left[(1+1/A)^n - 1\right]\right\}$
	$v_x^c = \dfrac{[(1+1/2n)\Delta h]^{1+1/n}}{1+1/n}\left[\dfrac{n(1-e^{-\alpha})/\alpha}{1/A^n - 1/(A+1)^n}\right]^{1/n}$	

The lower bound is the critical value at which no flow can occur in a converging channel: the expanding core touches the wall at the outlet and breaks at the inlet plane, i.e., $\sigma_1(0) = 1/2$ and $\sigma_1(1) = 0$. From Eq. (80), we get $A = -1$ and

$$(\Delta h)_{\min} = -\frac{1}{1 + \frac{1}{2n}}. \tag{89}$$

The upper bound is the critical value at which the contracting unyielded core in an expanding channel breaks at the outlet plane, while it touches the wall at the inlet plane, i.e., $\sigma_1(0) = 0$ and $\sigma_1(1) = (1 + \Delta h)/2$. In this case, Eq. (80) yields $A = 0$ and

$$(\Delta h)_{\max} = \frac{1}{1 + 1/n}. \tag{90}$$

In Bingham-plastic flow ($n = 1$), $-2/3 < \Delta h < 1/2$.

A. Critical Bingham numbers

In the case of a diverging channel ($\Delta h > 0$), $\sigma_1(x)$ is increasing, while $\sigma_2(x)$ is decreasing downstream. Therefore, the plug breaks at $x_c = 1$ and $C_c = (1 + 1/n)(1 + \Delta h)$, which gives

$$A_c = \frac{1 - (1 + 1/n)\Delta h}{(2 + 1/n)\Delta h}. \tag{91}$$

The first critical Bingham number is given by

$$Bn_{c1} = \frac{(1+1/n)\Delta h(1-I_c)}{2\int_0^1 g(\beta p)dx}, \tag{92}$$

where

$$I_c \equiv I(A_c) = \int_0^1 p_c(x)\,dx. \tag{93}$$

The flow stops when the two yield surfaces touch the walls at the inlet plane, $x_w = 0$. In this case, $C_w = 2 + 1/n$, which gives $A_w = 0$. For the second critical Bingham number, we get

$$Bn_{c2} = \frac{1}{2\int_0^1 g(\beta p_F)dx}, \tag{94}$$

where p_F is the pressure corresponding to a flat channel (of unit width). It should be noted that the integrals $\int_0^1 g(\beta p_F)dx$ have been already calculated in Table I, in order to derive the analytical expressions for the yield point σ. By means of Eq. (69), these can simply be deduced from Table I as the ratios σ/Bn. For example, when $f = g = 1 + x$,

$$\int_0^1 g(\beta p_F)dx = 1 - \beta\left[\frac{1}{\alpha} - \frac{1}{\ln(1+\alpha)}\right] \tag{95}$$

and therefore

$$Bn_{c2} = \frac{1}{2\left\{1-\beta\left[\frac{1}{\alpha} - \frac{1}{\ln(1+\alpha)}\right]\right\}}. \tag{96}$$

Similarly, for a converging channel ($\Delta h < 0$), $\sigma_1(x)$ is decreasing, while $\sigma_2(x)$ is increasing and thus the plug breaks at $x_c = 0$, $C_c = 1 + 1/n$, and

$$A_c = \frac{2}{(2+1/n)\Delta h}. \tag{97}$$

Hence

$$Bn_{c1} = \frac{(1+1/n)(-\Delta h)I_c}{2\int_0^1 g(\beta p)dx}. \tag{98}$$

The flow stops when the two yield surfaces touch the wall at the exit plane, $x_w = 1$, which yields $C_w = (2 + 1/n)(1 + \Delta h)$ and $A_w = -1$. Finally, the second critical Bingham number is given by

$$Bn_{c2} = \frac{1+\Delta h}{2\int_0^1 g(\beta p_F)dx}. \tag{99}$$

V. NUMERICAL RESULTS

All the results of this section have been obtained solving Eq. (51) numerically by means of central finite differences and considering only the Bingham-plastic case ($n = 1$) allowing only one of the two rheological parameters to vary linearly with pressure. The interval [0,1] has been partitioned uniformly using 1001 nodes. In the case of a linearly varying channel, the numerical results were found to be in excellent agreement with the semi-analytical solution derived in Sec. IV. It

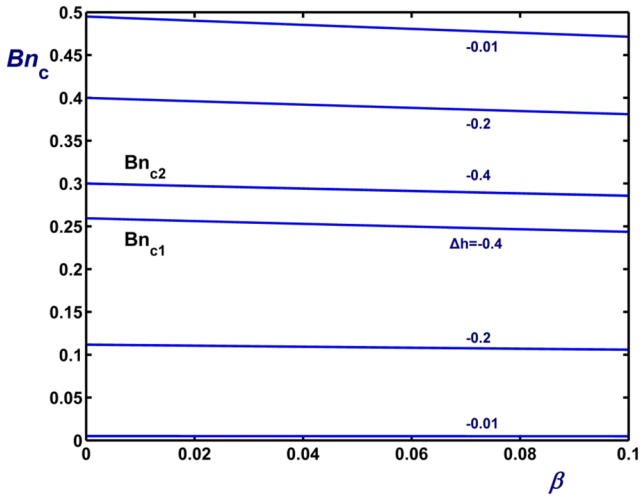

FIG. 2. Critical Bingham numbers for Bingham flow ($n = 1$) in an asymmetric converging channel ($h_1 = 0$, $h_2 = 1 + \Delta h$, $\Delta h < 0$) for $\alpha = 0$ (pressure-independent plastic viscosity).

should be noted that the latter solution requires the numerical solution of Eq. (78) for the constant A, which is not a straightforward task. In the case of linear g, we experimented with an iterative calculation of this constant by means of

$$A^{(m+1)} = \frac{1 + 2Bn\left[1 + \beta I(A^{(m)})\right] - (1+1/n)I(A^{(m)})\Delta h}{2 + 1/n}, \quad m = 0, 1, \ldots, \tag{100}$$

which is obtained by re-arranging Eq. (87). The numerical experiments showed that the above iterative method works very well except only when the Bingham number approaches Bn_{c2}. However, in these flows, the numerical method also

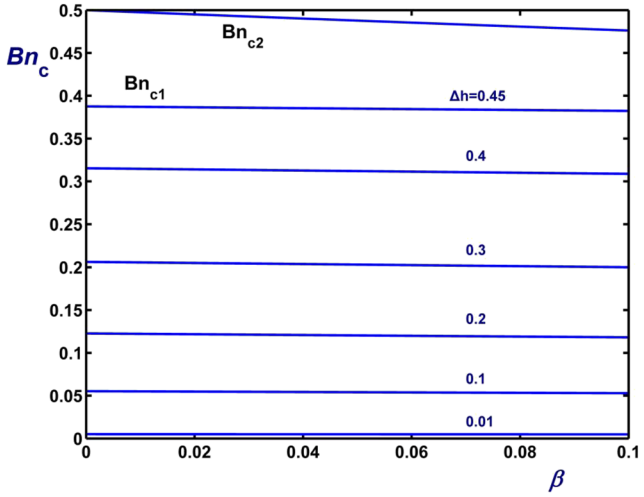

FIG. 3. Critical Bingham numbers for Bingham flow ($n = 1$) in an asymmetric diverging channel ($h_1 = 0$, $h_2 = 1 + \Delta h$, $\Delta h > 0$) for $\alpha = 0$ (pressure-independent plastic viscosity).

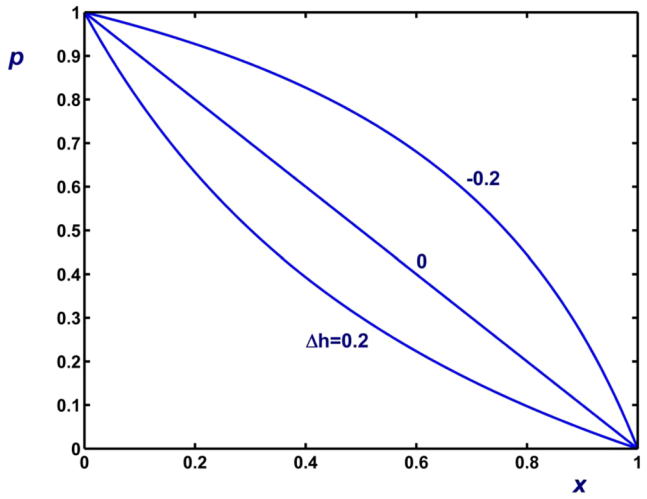

FIG. 4. Pressure distributions in Bingham flow (n = 1) in an asymmetric linearly varying channel with pressure-independent rheological parameters ($\alpha = \beta = 0$) and Bn = 0.2 for different values of Δh.

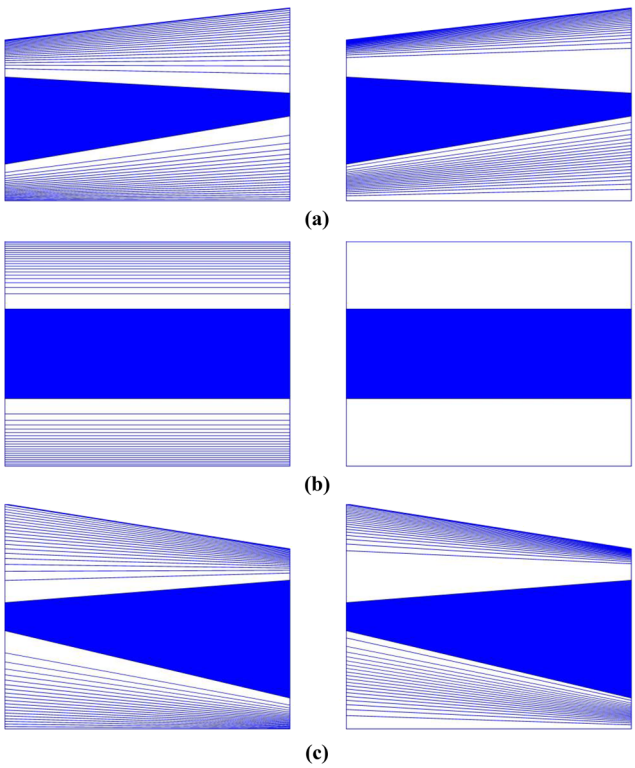

FIG. 5. Effect of Δh on the contours of the two velocity components (u_x in the left and u_y in the right column) in a linearly varying channel for Bn = 0.2, n = 1 (Bingham plastic), and $\alpha = \beta = 0$ (constant plastic viscosity and yield stress): (a) Δh = 0.2 (diverging channel), (b) Δh = 0 (flat channel), and (c) Δh = −0.2 (converging channel). The unyielded region is shaded.

encounters difficulties due to the very high pressure gradients in the regions where the unyielded core approaches the wall. These are resolved by means of finer partitions of the flow domain and parameter continuation.

In Fig. 2, we plot the critical Bingham numbers versus the yield-stress growth parameter β for different values of Δh in the case of flow of a Bingham fluid (n = 1) with pressure-independent plastic viscosity (α = 0) in a linearly converging channel ($\Delta h < 0$). It can be observed that the applicability window of the method becomes narrower as Δh tends toward the critical value of $-2/3$. In a diverging channel, Bn_{c2} is independent of Δh, as indicated also by Eq. (94). It is illustrated in Fig. 3 that as Δh tends to $(\Delta h)_{max} = 1/2$, Bn_{c1} increases approaching Bn_{c2} and limiting the applicability of the method. We can also

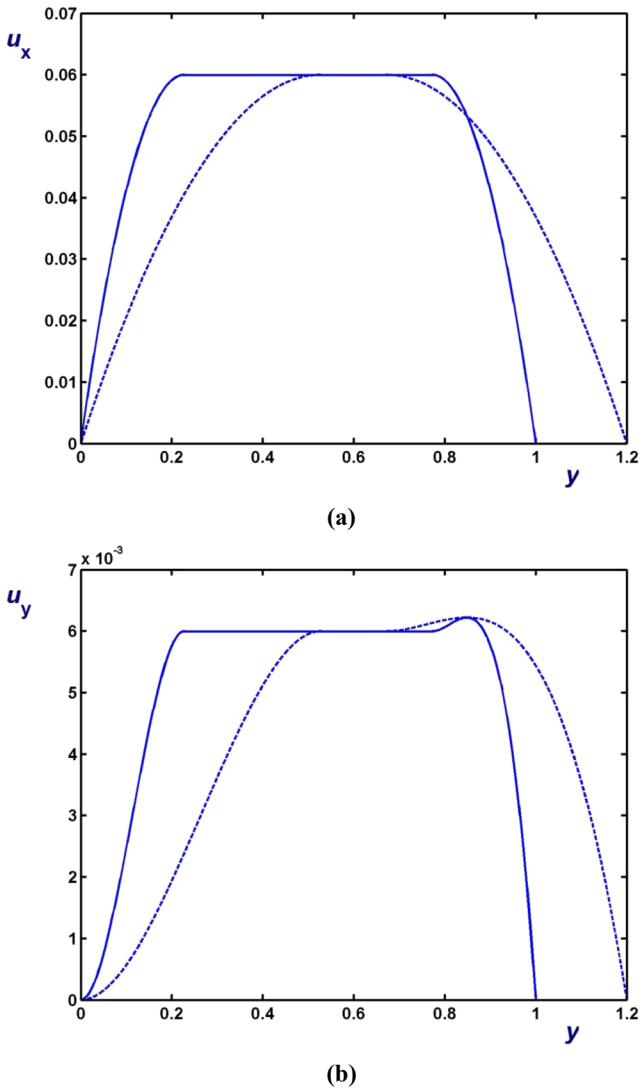

FIG. 6. Inlet (solid) and outlet (dashed) velocity profiles in the case of flow of a Bingham plastic (n = 1) in linearly diverging channel with Δh = 0.2 when Bn = 0.2 and $\alpha = \beta = 0$ (constant plastic viscosity and yield stress): (a) u_x and (b) u_y.

see in Figs. 2 and 3 that as Δh goes to zero (flat channel), Bn_{c1} tends to zero.

Figure 4 shows the pressure distributions for Bn = 0.2, $\alpha = \beta = 0$, and Δh = −0.2, 0 and 0.2. The pressure is linear in the case of a flat channel. In a converging channel, the pressure distribution is concave and the pressure gradient tends to zero at the inlet and to infinity at the outlet as Δh approaches the critical value of −2/3 at which the unyielded core touches the wall at the outlet plane and the flow ceases. In a diverging channel, the pressure distribution is convex and the pressure gradient tends to zero at the outlet and to infinity at the inlet as Δh approaches the critical value of 1/2 at which the unyielded core touches the wall at the inlet plane and the flow ceases. The velocity contours for the three geometries considered in Fig. 4 are shown in Fig. 5, where the shaded regions correspond to the unyielded core. The contours for 19 equidistant values in the range of the corresponding variable are drawn in all cases. As dictated by the analysis of the previous sections, the unyielded core in a flat channel is flat and converges in a diverging channel and vice versa. It should be noted that the horizontal velocity of the core is 0.0600, 0.045, and 0.030 for Δh = 0.2, 0, and −0.2, respectively, whereas the corresponding values of the transverse velocity are 0.0060, 0, and −0.0030, as dictated by Eq. (85). The absence of transverse velocity contour lines in the lower part of the upper yielded region indicates that the variation of this component is small there. Figures 6 and 7 show the profiles of the two velocity components at the inlet and the outlet planes for a Bingham plastic (n = 1) with constant rheological parameters ($\alpha = \beta = 0$) for Δh = 0.2 and −0.2, respectively. We observe that the distributions of u_y are characterized by a global extremum above the unyielded core, which is slightly higher than the positive core velocity in the diverging channel (Fig. 6) and slightly lower than the negative core velocity in the converging channel (Fig. 7).

The effect of the Bingham number on the pressure distribution in the case of a converging channel with Δh = −0.2 is illustrated in Fig. 8. Again, the rheological parameters are assumed to be pressure independent ($\alpha = \beta = 0$). As the Bingham number increases from $Bn = Bn_{c1}$ = 0.1118 toward Bn_{c2} = 0.4, the pressure gradient tends to zero near the inlet and to infinity near the exit. The velocity contours for $Bn = Bn_{c1}$, 0.25, and 0.35 are given in Fig. 9.

The effect of the plastic-viscosity growth number α for Bn = 0.25 and β = 0 on the pressure distribution is illustrated in Fig. 10. The values of α were taken to be rather high in order to magnify the effect of the parameter. As α increases, the pressure distribution tends to become linear, while the

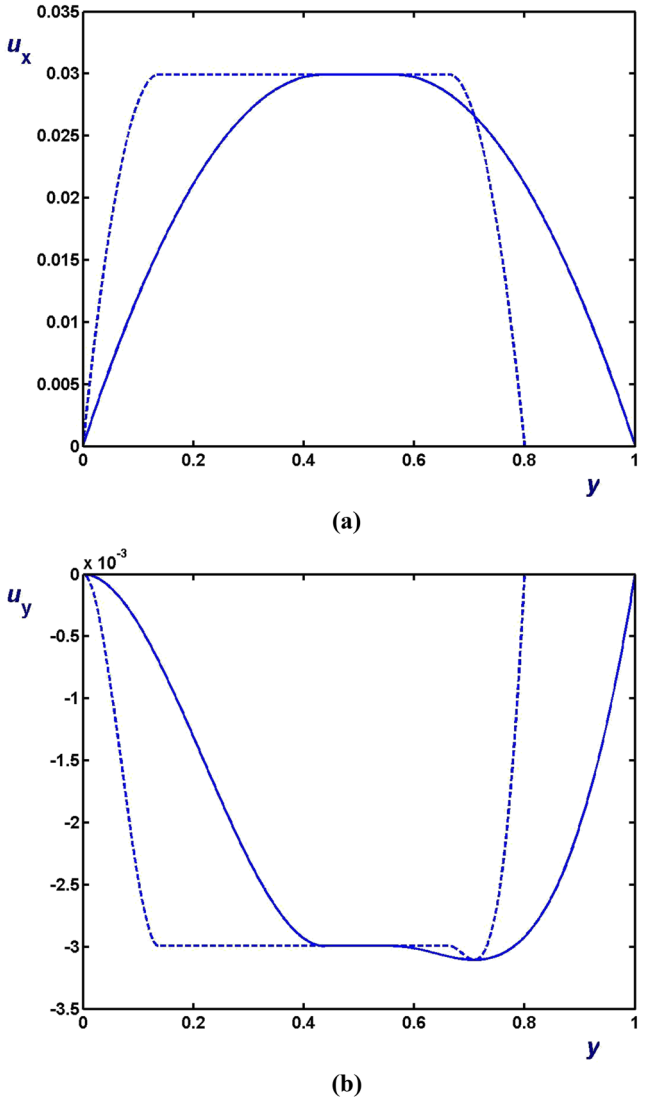

FIG. 7. Inlet (solid) and outlet (dashed) velocity profiles in the case of flow of a Bingham plastic (n = 1) in linearly converging channel with Δh = −0.2 when Bn = 0.2 and $\alpha = \beta = 0$ (constant plastic viscosity and yield stress): (a) u_x and (b) u_y.

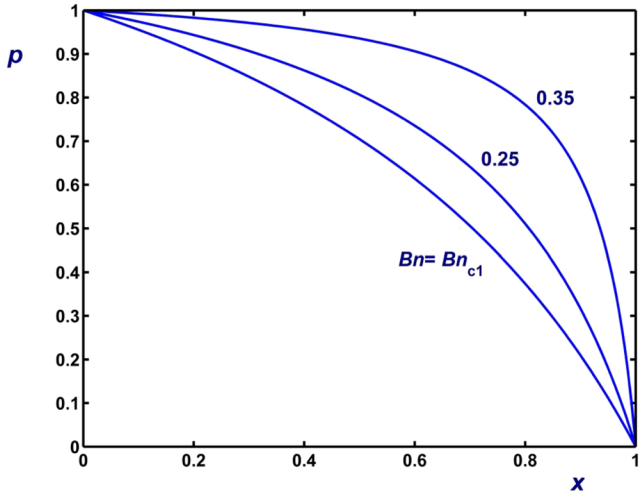

FIG. 8. Pressure distribution in Bingham flow (n = 1) in an asymmetric converging channel with Δh = −0.2 for various Bingham numbers and $\alpha = \beta = 0$ (pressure-independent rheological parameters).

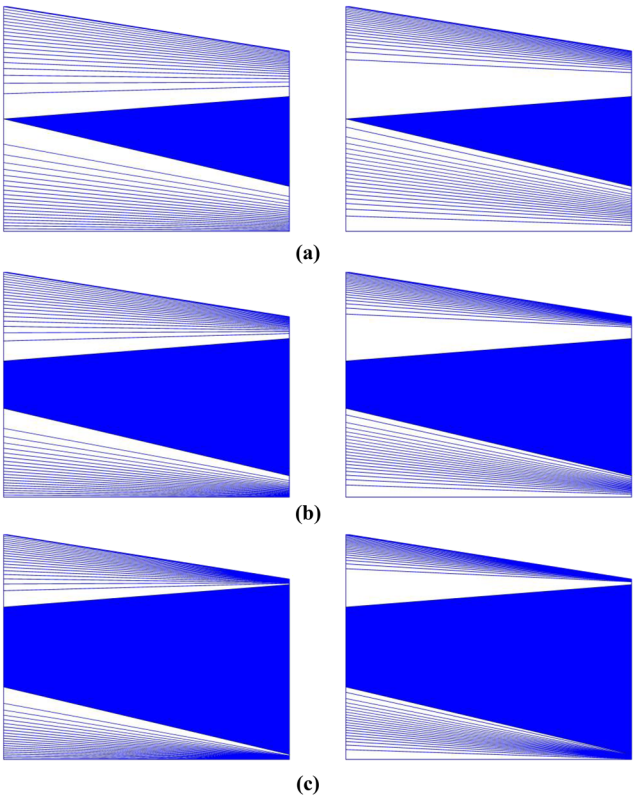

FIG. 9. Effect of the Bingham number on the contours of the two velocity components (u_x in the left and u_y in the right column) in a linear channel for $\Delta h = -0.2$, $n = 1$ (Bingham plastic), and $\alpha = \beta = 0$ (constant plastic viscosity and yield stress): (a) $Bn = Bn_{c1} = 0.1118$, (b) $Bn = 0.25$, and (c) $Bn = 0.35$. The unyielded region is shaded.

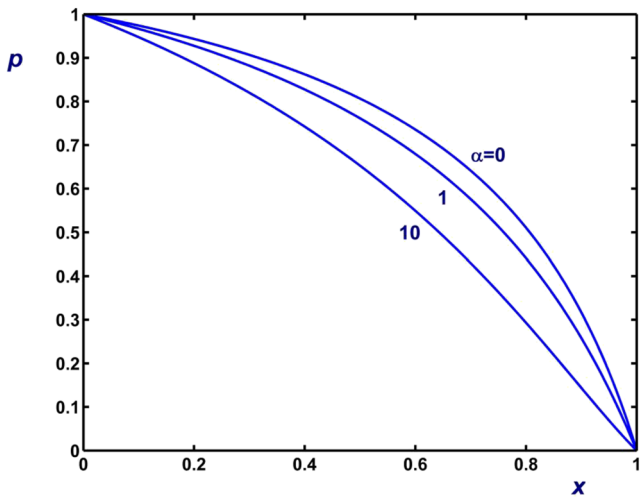

FIG. 10. Pressure distribution in Bingham flow ($n = 1$) in an asymmetric converging channel with $\Delta h = -0.2$, for $Bn = 0.25$, constant yield stress ($\beta = 0$) and different values of α.

unyielded core expands slightly, as can be observed in Fig. 11, where the velocity contours for the three cases of Fig. 10 are shown.

The effect of the yield-stress growth number β for $Bn = 0.25$ and $\alpha = 0$ is illustrated in Fig. 12. Again, rather high values of β are used, in order to enhance the differences. The effect of β is similar to that of the Bingham number, i.e., the pressure gradient increases very rapidly near the exit plane, and the unyielded core expands to eventually touch the walls at the exit (Fig. 13).

Results have also been obtained for geometries with nonlinear wall functions. Figures 14 and 15 show results obtained in a channel described by

$$h_1(x) = 0.02\sin(2\pi x), \quad h_2(x) = 1 - 0.02\sin(2\pi x) - 0.2x, \quad (101)$$

with $Bn = 0.2$, $a = 0$, and three values of the yield-stress growth coefficient, i.e., $\beta = 0$, 0.5, and 1. The pressure distributions are similar to those obtained for a linearly converging slide. However, the transverse velocity contours exhibit more interesting features. This is also the case with similar geometries, such as

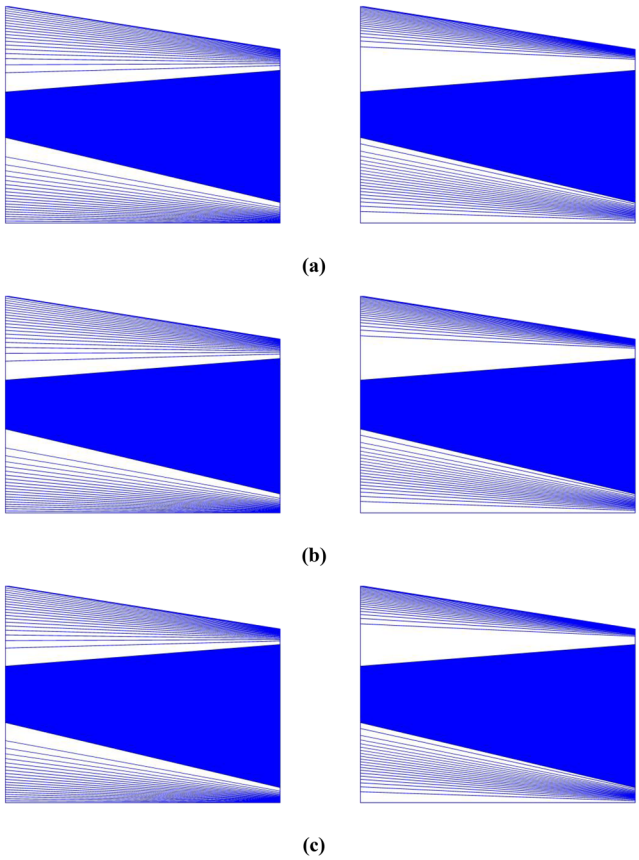

FIG. 11. Effect of α on the contours of the two velocity components (u_x in the left and u_y in the right column) in a converging channel ($\Delta h = -0.2$) for $Bn = 0.25$, $n = 1$ (Bingham plastic), $\beta = 0$ (constant yield stress): (a) $\alpha = 0$ (constant consistency index), (b) $\alpha = 1$, and (c) $\alpha = 10$. The unyielded region is shaded.

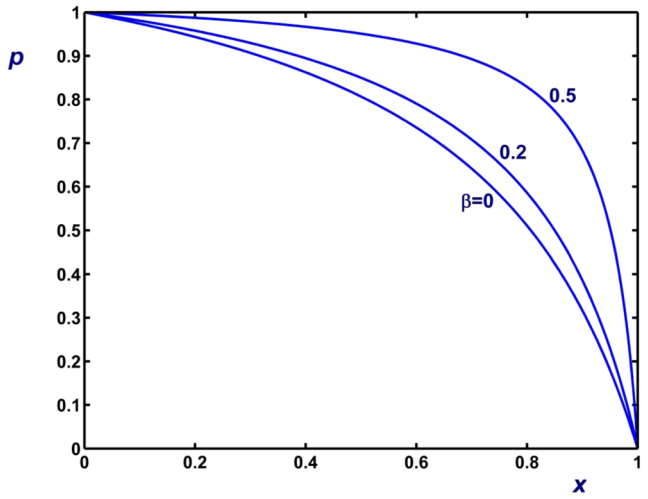

FIG. 12. Pressure distribution in Bingham flow (n = 1) in an asymmetric converging channel with $\Delta h = -0.2$, for Bn = 0.25, constant plastic viscosity (α = 0) and different values of β.

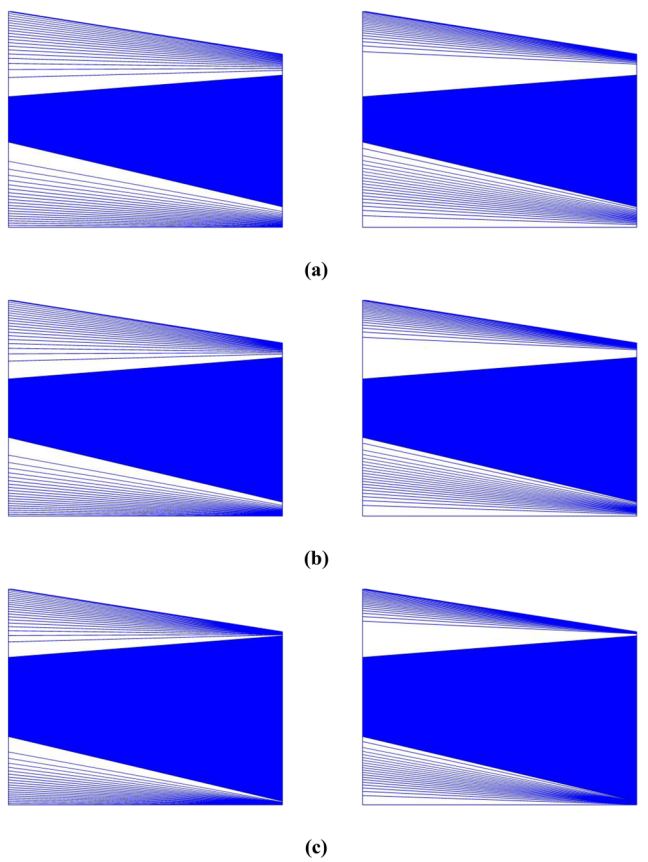

FIG. 13. Effect of β on the contours of the two velocity components (u_x in the left and u_y in the right column) in a converging channel ($\Delta h = -0.2$) for Bn = 0.25, n = 1 (Bingham plastic), α = 0 (constant plastic viscosity): (a) β = 0 (constant yield stress), (b) β = 0.2, and (c) β = 0.5. The unyielded region is shaded.

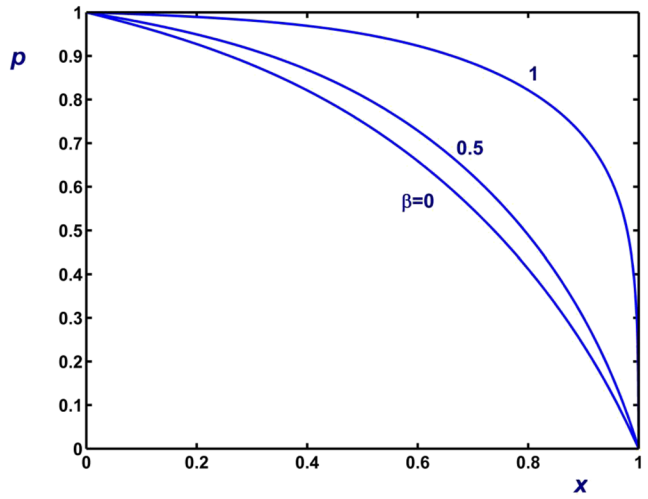

FIG. 14. Pressure distribution in Bingham flow (n = 1) in an asymmetric converging channel described by Eq. (101) for Bn = 0.2, constant plastic viscosity (α = 0), and β = 0, 0.5, and 1.

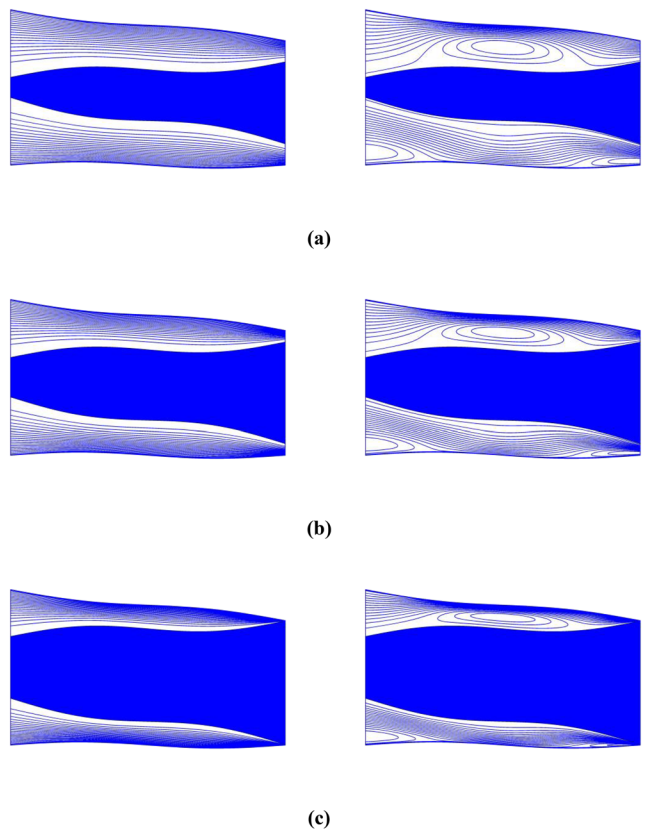

FIG. 15. Effect of β on the contours of the two velocity components (u_x in the left and u_y in the right columns) in an asymmetric channel described by Eq. (101) for Bn = 0.2, n = 1 (Bingham plastic), and α = 0 (constant plastic viscosity): (a) β = 0 (constant yield stress), and (b) β = 0.5, and (c) β = 1. The unyielded region is shaded.

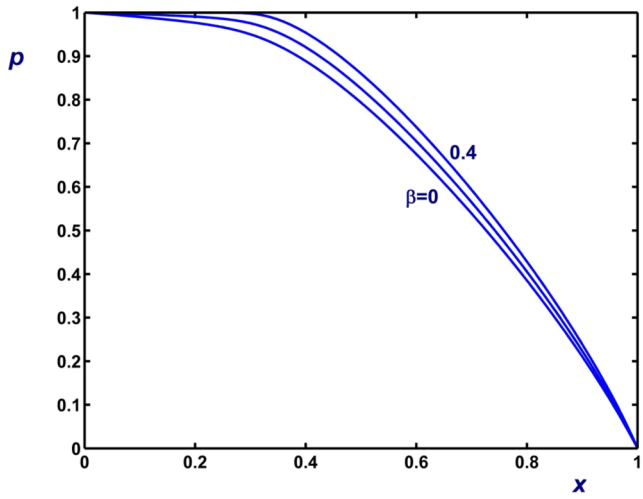

FIG. 16. Pressure distribution in Bingham flow ($n = 1$) in an asymmetric converging channel described by Eq. (102) for $Bn = 0.2$, constant plastic viscosity ($\alpha = 0$), and $\beta = 0$, 0.2, and 0.4.

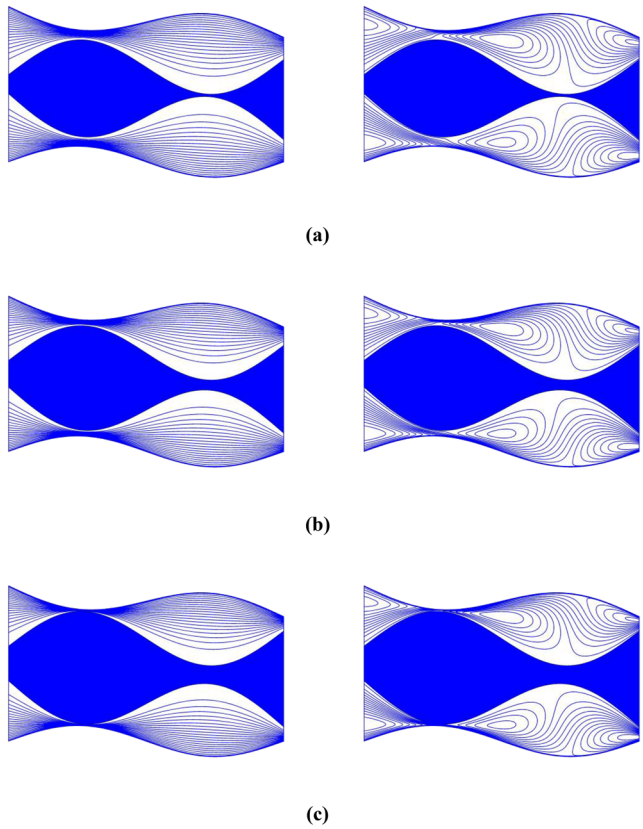

FIG. 17. Effect of β on the contours of the two velocity components (u_x in the left and u_y in the right columns) in an asymmetric channel described by Eq. (102) for $Bn = 0.2$, $n = 1$ (Bingham plastic), and $\alpha = 0$ (constant plastic viscosity): (a) $\beta = 0$ (constant yield stress), (b) $\beta = 0.2$, and (c) $\beta = 0.4$. The unyielded region is shaded.

that with

$$h_1(x) = 0.1\sin(2\pi x), \quad h_2(x) = 1 - 0.1\sin(2\pi x) - 0.2x. \tag{102}$$

The results in Figs. 16 and 17 have been obtained for $\beta = 0$, 0.2, and 0.4. It can be observed in Fig. 17, where the unyielded core is shown together with the velocity contours, that the value of the Bingham number ($Bn = 0.2$) is close to Bn_{c1} when $\beta = 0$ and gets closer to Bn_{c2} when $\beta = 0.4$, which simply means that the range of Bingham numbers in which the method is applicable is reduced with the yield-stress growth parameter. Recall, however, that the values of β have intentionally been chosen to be high in order to enhance the effects of this parameter.

VI. CONCLUSIONS

We have extended the lubrication approximation method of Fusi *et al.*[2] to analyze the flow of a Herschel-Bulkley fluid with pressure-dependent rheological parameters in a long, asymmetric channel described by two wall functions $h_1(x)$ and $h_2(x)$, under the assumption that the unyielded core extends from the inlet to the outlet plane of the channel. At zero order, the pressure obeys a first-order integrodifferential equation, which is numerically solved in the general case. Then the positions of the lower and upper yield surfaces as well as the two velocity components are calculated via closed-form analytical expressions. The applicability of the method is restricted to channels where the sum $h_1(x) + h_2(x)$ is a linear function of x and for Bingham numbers between the two critical values corresponding to the breaking of the plug region and to the complete cessation of the flow.

Our analysis revealed that unlike the symmetric case, the transverse velocity of the unyielded core is nonzero. Moreover, the widths of the lower and upper yielded regions are equal for any x and increase with the width of the channel, which implies that the width of the unyielded core increases if the width of the channel decreases and vice versa. The variation of the width of the unyielded core is enhanced by shear thinning and is independent of the other material and flow parameters.

Currently, we are exploring the possibility of applying the present model to non-inertial flows of single-phase yield-stress fluids along an asymmetric fracture[11] and to the upstream flow in sheet- or wire-coating.[12]

ACKNOWLEDGMENTS

Iasonas Ioannou gratefully acknowledges the support of the Onassis Foundation.

REFERENCES

[1] P. Panaseti, Y. Damianou, G. C. Georgiou, and K. D. Housiadas, "Pressure-driven flow of a Herschel-Bulkley fluid with pressure-dependent rheological parameters," Phys. Fluids **30**, 030701 (2018).

[2] L. Fusi, A. Farina, F. Ross, and S. Roscani, "Pressure-driven lubrication flow of a Bingham fluid in a channel: A novel approach," J. Non-Newtonian Fluid Mech. **221**, 66–75 (2015).

[3] C. Barus, "Isothermals, isopiestics and isometrics relative to viscosity," Am. J. Sci. **45**, 87–96 (1893).

[4]I. R. Ionescu, A. Mangeney, F. Bouchut, and O. Roche, "Viscoplastic modeling of granular column collapse with pressure-dependent rheology," J. Non-Newtonian Fluid Mech. **219**, 1–18 (2015).
[5]J. Hermoso, F. Martinez-Boza, and C. Gallegos, "Combined effect of pressure and temperature on the viscous behaviour of all-oil drilling fluids," Oil Gas Sci. Technol. - Rev. IFP Energies Nouv. **69**, 1283–1296 (2014).
[6]I. A. Frigaard and D. P. Ryan, "Flow of a visco-plastic fluid in a channel of slowly varying width," J. Non-Newtonian Fluid Mech. **123**, 67–83 (2004).
[7]A. Putz, I. A. Frigaard, and D. M. Martinez, "On the lubrication paradox and the use of regularization methods for lubrication flows," J. Non-Newtonian Fluid Mech. **163**, 62–77 (2009).
[8]K. D. Housiadas, I. Ioannou, and G. C. Georgiou, "Lubrication solution of the axisymmetric Poiseuille flow of a Bingham fluid with pressure-dependent rheological parameters," J. Non-Newtonian Fluid Mech. **260**, 76–86 (2018).
[9]L. Fusi and A. Farina, "Peristaltic axisymmetric flow of a Bingham plastic," Appl. Math. Comput. **320**, 1–15 (2018).
[10]L. Fusi, "Channel flow of viscoplastic fluids with pressure-dependent rheological parameters," Phys. Fluids **30**, 073102 (2018).
[11]A. Roustaei, T. Chevalier, L. Talon, and I. A. Frigaard, "Non-Darcy effects in fracture flows of a yield stress fluid," J. Fluid Mech. **805**, 222–261 (2016).
[12]M. M. Denn, *Polymer Melt Processing* (Cambridge University Press, Cambridge, 2008).